Cationic Fluoropolyphosphazenes: Synthesis and Assembly with Heparin as a Pathway to Hemocompatible Nanocoatings

Alexander Marin, ¹ Jordan Brito, ² Svetlana A. Sukhishvili, ² Alexander K. Andrianov*, ¹

¹Institute for Bioscience and Biotechnology Research, University of Maryland, Rockville, MD

²Department of Materials Science & Engineering, Texas A&M University, College Station, TX

KEYWORDS: fluoropolymers; polyphosphazenes; layer-by-layer; anticoagulant; hemocompatible

ABSTRACT: The development of state-of-the-art blood-contacting devices can be advanced through integrating hemocompatibility, durability, and anticoagulant functionalities within engineered nano-scale coatings. To enable all-aqueous assembly of nanocoatings combining omniphobic fluorinated features with the potent anticoagulant activity of hydrophilic heparin, two fluoropolymers containing cationic functionalities were synthesized - poly[(trifluoroethoxy)(dimethylaminopropyloxy)phosphazene], PFAP-O and poly[(trifluoroethoxy)(dimethylaminopropylamino)phosphazene], PFAP-A. Despite a relatively high content of fluorinated pendant groups — approximately 50% (mol) in each — both polymers displayed solubility in aqueous solutions and were able to spontaneously form stable supramolecular complexes with heparin, as determined by dynamic light scattering (DLS) and asymmetric flow field flow fractionation (AF4) methods. Heparin-containing coatings were then assembled by layer-by-layer deposition in aqueous

solutions. Nano-assembled coatings were evaluated for potential thrombogenicity in three important categories of in vitro tests - coagulation by thrombin generation, platelet retention, and hemolysis. In all assays, heparin-containing fluoro-coatings consistently displayed superior performance compared to untreated titanium surfaces or fluoro-coatings assembled using poly(acrylic acid) in the absence of heparin. Short-term stability studies revealed the non-eluting nature of these non-covalently assembled coatings.

INTRODUCTION

The development of advanced materials for blood-contacting medical devices faces challenges associated with activation of blood defense mechanisms, such as triggering coagulation cascade, activation of complement system and cellular inflammatory mechanisms.¹⁻⁵ Despite the fact that some advanced materials are efficient in reduction of cell adhesion and protein adsorption, there are presently no clinically available biomaterials which can entirely inhibit thrombosis under challenging physiological environments, such as in a low-pressure venous system.¹

Surface grafting of an anticoagulant drug - heparin - is one of the most viable and effective approaches in reducing thrombosis and thromboembolic complications, which may be triggered by biomaterials.^{1, 4, 5} Approximately a dozen of commercially marketed medical devices with functionally active heparin coatings have been developed with the absolute majority of them using covalent immobilization of the drug.^{5, 6} Alternatively, heparin was also assembled at surfaces ionically using the layer-by-layer (LbL) technique, which enables all-aqueous deposition of nanocoatings of controlled thickness onto surfaces of a variety of shapes and chemistries.⁷ Using LbL deposition, heparin was immobilized on the surface of silk with cationic poly(allylamine hydrochloride) as an ionic partner, yielding highly hydrophilic surfaces displaying strong resistance to platelet adhesion.⁸ Attempts to combine heparin-enabled antithrombotic functionality with the durability and antibacterial properties of fluoro- surfaces⁹⁻¹¹ have been also

undertaken. However, preparation of such coatings has been only achieved via multi-step sophisticated processes, such as fluoro-silanization of silicon surface with subsequent photo-initiated attachment of azido-modified heparin¹² or surface grafting of fluoropolymer using poly(acrylic acid) with covalently attached heparin.¹³

We have previously introduced a family of water-soluble polyphosphazene polyanions, which contained fluorinated side groups and have been successfully employed to produce nano-coatings from aqueous solutions using LbL deposition technique. 14-19 These fluoro-coatings displayed remarkable biocompatibility and bactericidal activity. Here, we aimed to additionally impart antithrombotic activity to this type of ionic nano assemblies by including negatively charged heparin into such nanofilms. To that end, a new cationic fluoropolymer capable of LbL assembly in aqueous solutions needed to be developed.

Cationic fluoropolymer systems have been gaining attention largely due to their ability to dramatically enhance efficiency of intracellular gene and protein delivery. Some fluorinated polyacrylates were also used as surface coating agents and have been shown to enhance antibacterial activity and bacterial antiadhesion compared to their non-fluorinated counterparts. However, practically all reported polymers either bear relatively low content of fluorine or are not soluble in aqueous solutions. Therefore, to date the use of cationic fluoropolymers in various applications has been limited to nanomicelles and nanoparticles, dendrimers, and solvent-cast films.

Here, we introduce two novel water-soluble polyphosphazenes, which bear fluoro- and cationic functionalities - poly[(trifluoroethoxy)(dimethylaminopropyloxy)phosphazene], PFAP-O and poly[(trifluoroethoxy)(dimethylaminopropylamino)phosphazene], PFAP-A. Both polymers displayed water-solubility and were able to assemble with heparin in aqueous solutions, with PFAP-O showing the superior ability to form nanofilms using the LbL technique. In vitro thrombogenicity studies were conducted to demonstrate antithrombotic activity and excellent hemocompatibility of nanofilms.

MATERIALS AND METHODS

Materials. 3-Dimethylamino-1-propylamine (Acros Organics, Morris Plains, NJ); 3-dimethylamino-1-propanol; 2,2,2-trifluoroethanol; sodium hydride; bis(2-methoxyethyl) ether, diglyme; triethylamine; heparin sodium salt from porcine intestinal mucosa; branched polyethyleneimine (750 kDa); poly(acrylic acid) (450 kDa); titanium foil; nicotinamide adenine dinucleotide, reduced disodium salt hydrate - NADH, sodium pyruvate, Triton X-100 (Sigma-Aldrich, Saint Louis, MO) were used as received. Boron-doped silicon wafers were purchased from University Wafer, Inc. Polydichlorophosphazene (PDCP) was synthesized as described previously²⁷ and the same lot was used to synthesize both polymers.

Physico-Chemical Characterization Methods. ¹H NMR and ³¹P NMR spectra were recorded using 400 MHz Ascend[™] Bruker NMR spectrometer (Bruker Biospin Corp, Billerica, MA). Dynamic light scattering measurements were conducted using Malvern Zetasizer Nano series instrument (Malvern Instruments Ltd., Worcestershire, UK). Asymmetric flow field flow fractionation, AF4 analysis was carried out using a Postnova AF2000 MT instrument (Postnova Analytics GmbH, Landsberg, Germany).

Synthesis of poly[(2,2,2-trifluoroethoxy)(3-dimethylamino-1-propyloxy)phosphazene], PFAP-O. All reactions were carried out under an atmosphere of anhydrous nitrogen either using MBraun Labstar Pro glovebox workstation (M. Braun Inertgas-Systeme Gmbh, Garching, Germany), or air-free laboratory techniques. A suspension of 0.145 g (6.05 mmol) sodium hydride in 5 mL of diglyme was slowly added to 0.46 mL (6.25 mmol) of 2,2,2-trifluoroethanol dissolved in 10 mL of diglyme. The resulting salt was added dropwise to 0.7 g (6 mmol) of PDCP in 25 mL of diglyme. The reaction was kept at ambient temperature under stirring for 5 h. Then, a mixture of 4.26 mL (36 mmol) of 3-dimethylamino-1 propanol, 2.2 mL (15.6 mmol) of triethylamine, and 20 mL of diglyme was slowly added to the reaction flask. The reaction was let to continue under stirring at ambient temperature for 3 days. The reaction mixture then was placed in the freezer and kept overnight at -30 °C. The resulting precipitate was collected by centrifugation, rinsed with acetone, and air dried. The material was then dissolved in deionized water, which was adjusted to pH 5 with 1 N hydrochloric acid, dialyzed against water using Repligen biotech cellulose ester dialysis

tubing, 50 kDa molecular weight cutoff (Spectrum Chemical, New Brunswick, NJ), and then lyophilized. Polymer yield - 0.75 g (51%).

¹H NMR (400 MHz, methanol d4): δ [ppm]: 4.2 ppm (br, 2H, -CH₂-CF₃); 3.3 ppm (br, 2H, -O-CH₂-C); 2.9 ppm (br, br, 8H, $-CH_2-N(CH_3)_2$); 2.1 (br, 2H, C- CH_2-C). ³¹P NMR (162 MHz, methanol-d4): (δ [ppm]: -4 ppm. **Synthesis** of PFAP-A. **Synthesis** of poly[(2,2,2-trifluoroethoxy)(3-dimethylamino-1propylamino)phosphazene], PFAP-A. The synthesis and purification of PFAP-A was carried out similarly; however, 3-dimethylamino-1-propylamine was used instead of 3-dimethylamino-1-propanol. The following amounts of reagents were employed. Partial substitution was conducted by adding sodium trifluoroethoxide, which was prepared by combining 0.157 g (6.5 mmol) of sodium hydride in 5 mL of diglyme with 0.5 mL (6.76 mmol) of 2,2,2-trifluoroethanol in 10 mL of diglyme, to 6.5 mmol (0.75 g) PDCP dissolved in 25 mL of diglyme. Then, 4.56 ml (39 mmol) of 3-dimethylamino-1 propylamine and 2.4 mL (16.9 mmol) of triethylamine in 20 mL diglyme were used to complete the substitution as described above. Yield - 0.71 g (45%).

¹H NMR (400 MHz, methanol d4): δ [ppm]: 4.1 ppm (br, 2H, -C $\underline{\mathbf{H}}_2$ -CF₃); 3.2 ppm (br, 2H, =N-C $\underline{\mathbf{H}}_2$ -C); 2.8 ppm (br, 8 $\underline{\mathbf{H}}$, -C $\underline{\mathbf{H}}_2$ -N(C $\underline{\mathbf{H}}_3$)₂); 2.0 ppm (br, 2H, -C-C $\underline{\mathbf{H}}_2$ -C-); 1.1 ppm (1H, -N $\underline{\mathbf{H}}$ -C). ³¹P NMR (162 MHz, methanol-d4) δ [ppm]: -6 ppm.

Layer-by-Layer Deposition. Films were deposited using the dip-deposition technique. To prepare for LbL deposition, silicon wafers and titanium foil were cut into 1.2 × 1.2 cm pieces, cleaned by overnight exposure to UV light, and soaked in a concentrated sulfuric acid bath for 40 min to clean and introduce charged groups to the surface. Solutions of heparin, poly(acrylic acid), and PFAP-O were prepared by dissolving in Milli-Q water (0.4 mg/mL) and adjusting to pH 7.5 by additions of 0.1 or 0.01 M NaOH or HCl. As described elsewhere, substrates were primed with a monolayer of branched polyethyleneimine at pH 9 for 15 minutes and rinsed with Milli-Q water. Then, layers of anion (poly(acrylic acid) or heparin) and PFAP-O were alternately deposited on the wafer by soaking in solutions for 5 min, finally capping the

film with either poly(acrylic acid) or heparin. Each deposition cycle was followed by a water rinsing step to remove excess material.

Spectroscopic Ellipsometry. The thicknesses and refractive indices of the LbL coatings on silicon were characterized using a M-2000 automated-angle spectroscopic ellipsometer (J.A. Woollam Co., Inc.). Dry film measurements were collected at four incidence angles: 45° , 55° , 65° , and 75° . To fit the ellipsometric data, the dry LbL coating on silicon was treated as a Cauchy material of thickness d atop a silicon and native oxide layer. Fitting coefficients and thickness d were fitted simultaneously as described previously.²⁹

Thrombin Generation Assay (TGA). Thrombin generation was assayed using a fluorometric detection method. Human citrated plasma was obtained by centrifugation of the whole blood (Innovative Research, Inc., Novi, MI) at 2,000 g for 10 min. Test articles (1.2x1.2 cm) were first incubated with 150 μ L of plasma at 37°C for 10 min. Thrombin formation was started by adding 50 μ L of 15 mM calcium chloride solution in PBS. Samples were incubated at 37°C for 5 min and 10 μ L of plasma solution was transferred to 250 μ L 50 mM Tris buffer (pH 7.4) to stop the reaction. Then 20 μ L of fluorogenic thrombin substrate III - Calbiochem (Sigma-Aldrich, Saint Louis, MO) solution (0.2 mg/mL in 90% 50 mM Tris buffer and 10% DMSO) was added. Thrombin activity was determined by measuring fluorescence of solution (λ ex 360 nm, λ em 465 nm) and expressed as intensity after 10-, 20-, and 30-min reaction time.

Platelet Adhesion. Retention of platelets on surfaces was assayed by measuring the enzymatic activity of lactate dehydrogenase (LDH) released after surfactant-induced cell lysis. ³⁰ Specifically, test articles were incubated with 150 μL of platelet rich plasma (PRP) obtained from whole human blood (Innovative Research, Inc., Novi, MI) by centrifugation (100 g, 20 min) at 37°C for 45 min and then rinsed with PBS (pH 7.4) to remove any unbound platelets. Lysis of surface-adhered cells and the release of LDH was induced by adding 100 μL of 1 % (w/v) aqueous Triton X-100 solution to rinsed samples. After 5 min of incubation, 50 μL of lysate was collected and 200 μL of an aqueous mixture of 0.28 mg/mL NADH and 0.17 mg/mL sodium pyruvate in 80 mM Tris buffer containing 200 mM sodium chloride (pH 7.2) was added to the

lysate. LDH activity was measured photometrically at 340 nm for 60 min and expressed as NADH consumption in the enzymatically catalyzed conversion of pyruvate to lactate. The number of adherent platelets was proportional to consumed NADH or LDH activity of the lysate.

Hemolysis. Hemolysis of diluted human blood on coated and uncoated titanium samples was evaluated using a modified American Society for Testing and Materials (ASTM) method, which monitors the released amount of hemoglobin. Specifically, whole human blood in sodium citrate (Innovative Research, Inc., Novi, MI) was diluted with PBS 50-fold. Test articles (1.2 x 1.2 cm) were incubated with 1 mL of diluted blood at 37 °C for 4 h. The suspensions were then centrifuged for 5 min (14 000 rpm) and the concentration of hemoglobin in the supernatant was analyzed by UV–VIS spectrophotometry using hemoglobin calibration curves obtained at 380, 415, and 450 nm (Multiscan Spectrum microplate spectrophotometer, ThermoFisher Scientific, Waltham, MA). Total hemoglobin concentration in samples before incubation was determined assuming that 100 % lysis was achieved by 100-fold dilution of samples with ultrapure water. The percent of hemolysis was calculated as a ratio between the hemoglobin concentration in samples after and before incubation of blood with test articles. All samples were analyzed in triplicate.

Stability Studies. Stability of coated samples was evaluated by incubating them in PBS (pH 7.4) at 37°C for up to three weeks and measuring their anticoagulation activity using TGA, as described above. Samples (1.2x1.2 cm) were submerged in PBS for various periods of time, then washed with deionized water, dried by compressed air and incubated with Human plasma to analyze their activity by TGA. The maximum slope on the "fluorescent intensity vs time" graph was used to compare anticoagulant activity of heparincontaining samples. Analysis was conducted in duplicates.

RESULTS AND DISCUSSION

Synthesis and Characterization of Cationic Fluoro-Polyphosphazenes. Fluoropolymers containing cationic functionalities were designed to include tertiary amino groups linked to phosphazene backbone either via oxy- (PFAP-O) or amino- (PFAP-A) bridges (Scheme 1). This two-pronged structural approach was primarily dictated by previously reported challenges in the synthesis of non-fluorinated polyphosphazenes with either dimethylaminoethylamino²⁵ or dimethylaminoethoxy³² side groups. Furthermore, to minimize the possibility of synthetic difficulties associated with suggested side group rearrangements, which allegedly involved dimethylaminoethyl derivatives, ³² dimethylaminopropyl side groups were chosen.

Scheme 1. Synthetic pathways for PFAP-O and PFAP-A.

Synthesis of polymers was conducted via a macromolecular substitution route by sequential modification of PDCP with 2,2,2-trifluoroethanol followed by reactions with either 3-dimethylamino-1-propanol, or 3-dimethylamino-1-propylamine (**Scheme 1**). This order of reagent addition, which provided the same partially fluoro- substituted PDCP as a precursor for the synthesis of both polymers, was chosen to achieve similar side group substitution patterns.

Structures of both polymers were confirmed by ¹H NMR (**Figures S1-S2**) with the 1:1 molar ratio between fluorinated and amino groups (**Table 1**). ³¹P NMR spectra revealed unresolved broad peaks for either polymer (**Figures S3-S4**), which is consistent with previously reported observations for water-insoluble polyphosphazene copolymers containing dimethylethylamino groups (reported broad peaks, centers of peaks between 5 and 7.5 ppm).²⁵

In order to evaluate the molecular masses of copolymers, gel permeation chromatography (GPC) analysis was undertaken, but the apparent strong interactions of these polymers with the resin of the column prevented its elution. Attempts to resolve the issue by varying composition of the mobile phase and column priming were unsuccessful. This is consistent with prior reports that GPC analysis of

hydrophobically modified cationic polymers, which have a tendency for aggregation and flocculation, has been notoriously difficult. 33, 34 Therefore, the molecular weights were assessed by alternative methods – dynamic light scattering (DLS) and asymmetric flow field-flow fractionation (AF4) measurements using water-soluble polyphosphazene standards, which were characterized as described previously.³⁵ Note that hydrodynamic dimensions of polymers determined by DLS were earlier successfully correlated with their molecular masses determined using GPC with static light scattering detection or analytical ultracentrifugation.^{36, 37} Here, the DLS molecular masses were evaluated from the diameter-molecular mass calibration curves using z-average hydrodynamic diameters (Figure S5) and are shown in Table 1. Furthermore, the analysis of molar masses was conducted using an AF4 method. This method is similar to GPC as it allows separation of macromolecules on the basis of their molecular dimensions. However, compared to GPC, interactions with the stationary phase are further minimized as separation is achieved by applying a cross-flow of a mobile phase against the surface of a semi-permeable membrane.³⁸ The applicability of this method to the molecular mass analysis of polymers has been also successfully demonstrated previously. 33, 39 Figure S6 shows AF4 fractograms of both fluorinated polymers along with representative profiles of the molecular standards and the calibration curve. AF4 results were in agreement with DLS measurements indicating that the molecular masses of both polymers were in excess of 100 kDa and the molecular mass of PFAP-O was somewhat higher than that of PFAP-A (Table 1). Nevertheless, molar masses obtained by AF4 analysis were higher than those determined by DLS. The approximately two-fold difference is likely due to the delayed elution of polymers due to interactions with the semi-permeable membrane. This is consistent with some 'tailing' visible on the left side of fractograms of both polymers (Figures S6A and S6B) and is in line with the ability of these polymers to strongly interact with the stationary phase, which was observed by GPC analysis.

Table 1. Physico-chemical characterization of cationic fluoropolyphosphazenes.

		PFAP-O	PFAP-A
Composition,* % mol	O CH ₂ N CH ₃ CH ₂ CH ₂ CH ₃	50	-
	NH CH ₂ N CH ₂ CH ₃	-	49
	O _{CH2} CF ₃	50	51
Solution dimensions	D _h **, nm	41 (+/- 4)	28 (+/-2)
	Pdi***	0.4 (+/- 0.03)	0.6 (+/- 0.15)
Molecular Masses****	Mp, kDa (AF4)	510	210
	M _p , kDa (DLS)	310	120

^{*} calculated on the basis of 1H NMR analysis; ** D_h - z-average hydrodynamic diameter; *** Pdi - polydispersity index (D_h and Pdi are determined by DLS; 50 mM phosphate buffer; pH 7.4, 1 mg/mL polymer; standard deviation is shown in parenthesis; n=5); **** M_p - peak average molar mass determined by AF4 and DLS methods

Water-soluble Fluoropolymers Show Differences in pH-Dependent Solution Behavior. Despite a high content of hydrophobic trifluoroethoxy side groups, both PFAP-O and PFAP-A formed clear solutions in aqueous media in a wide pH range (conditions tested: pH 3-9; 0.05 to 5 mg/mL polymer concentration, 50 mM acetate and phosphate buffers), enabling their use as materials for LbL nanoassembly. However, DLS studies revealed some distinct differences in the solution behavior of these two polymers in response to pH changes. PFAP-O was characterized by an essentially monodisperse size distribution with a peak hydrodynamic diameter and polydispersity index of approximately 60 nm and 0.4, correspondingly, when analyzed in phosphate buffer in the pH range of 4-7.4 (Figure 1, solid lines). Further increase to pH 8 resulted in a detectable shift towards larger sizes with a peak diameter in the excess of 100 nm. This reveals some reversible agglomeration in the system, which is expected for a polymer with a large content of hydrophobic trifluoroethoxy groups and can be attributed to the loss or significant reduction of charges under basic conditions.

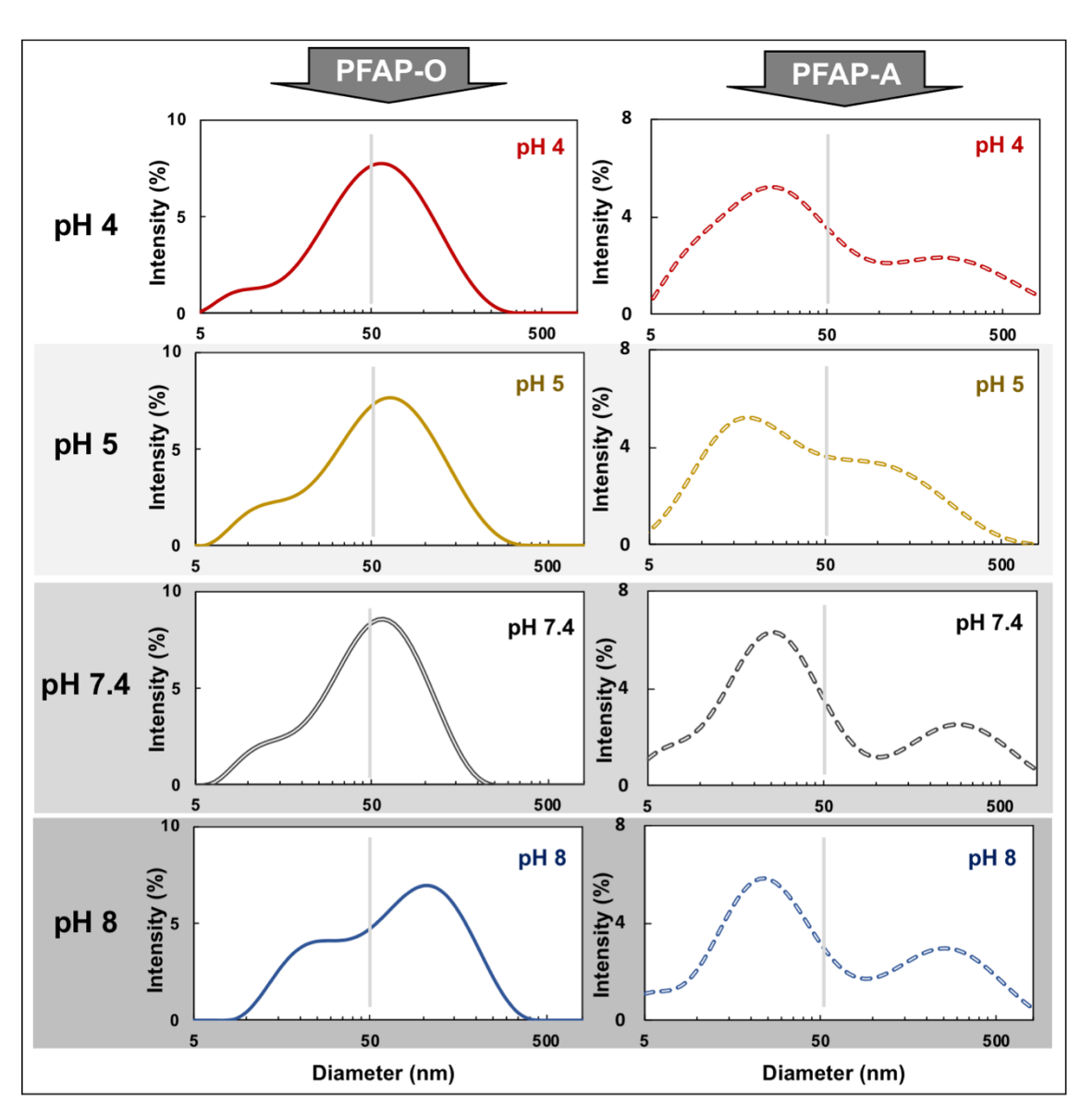


Figure 1. DLS profiles of PFAP-O (solid lines) and PFAP-A (dashed lines) in aqueous solutions of various pH (1 mg/mL polymer; 50 mM phosphate buffer).

In contrast, the DLS profiles observed for PFAP-A showed bimodality and had a significantly larger polydispersity index of 0.5-0.8 (**Figure 1**, dashed lines). Broad, pH-dependent variations in the diameter of the larger peak (100-400 nm) and varying ratios between the intensities of two peaks suggest reversible agglomeration of this polymer in solution, rather than the presence of chemically cross-linked microgels. The observed differences in solution behavior of the two polymers indicate that although both fluoropolymers form visibly clear solutions in aqueous media, PFAP-A is more susceptible to

agglomeration than PFAP-O. These dissimilarities between the two macromolecules can be either associated with their structural differences or caused by distinctions in their microtacticity. Although care was taken to select a synthetic pathway in which amino groups were only introduced in the last step of the macromolecular substitution, side group exchange reactions in polyphosphazene chemistry have been previously reported, ⁴⁰ and precise control of substitution patterns remains challenging.

Interactions of Fluoropolymers with Heparin in Aqueous Solutions. The ability of fluoropolymers to spontaneously self-assemble with heparin was studied in aqueous solutions by DLS. Compositiondependent changes in hydrodynamic diameter of heparin-polymer formulations, along with representative DLS profiles, are shown in Figure 2A. It is seen that both polymers undergo agglomeration in the presence of heparin, indicating formation of complexes. However, the onset of agglomeration for PFAP-A was observed at a lower concentration of heparin, likely due to greater susceptibility of this polymer to agglomeration mentioned above. The formation of heparin-polymer complexes was further analyzed by the AF4 method by monitoring concentration of unbound heparin in the system. AF4 fractograms and resulting isotherms of binding confirm the formation of complexes and reveal similar profiles for both polymers, although PFAP-O appeared to uptake more polysaccharide (Figures 2B and \$7). The assessment of dissociation constants was conducted on the basis of a simplified binding model by determining concentration of heparin at a half-saturation of polymers.⁴¹ The values in the micromolar range (3x10⁻⁶ and 7x10⁻⁶ for PFAP-A and PFAP-O, respectively) suggest high stability of the complexes. Note that biologically important non-covalent interactions usually range from picomolar/nanomolar for the tightest interactions, to millimolar for the weakest, with micromolar values typical for binding of signaling protein to a biological target.⁴¹

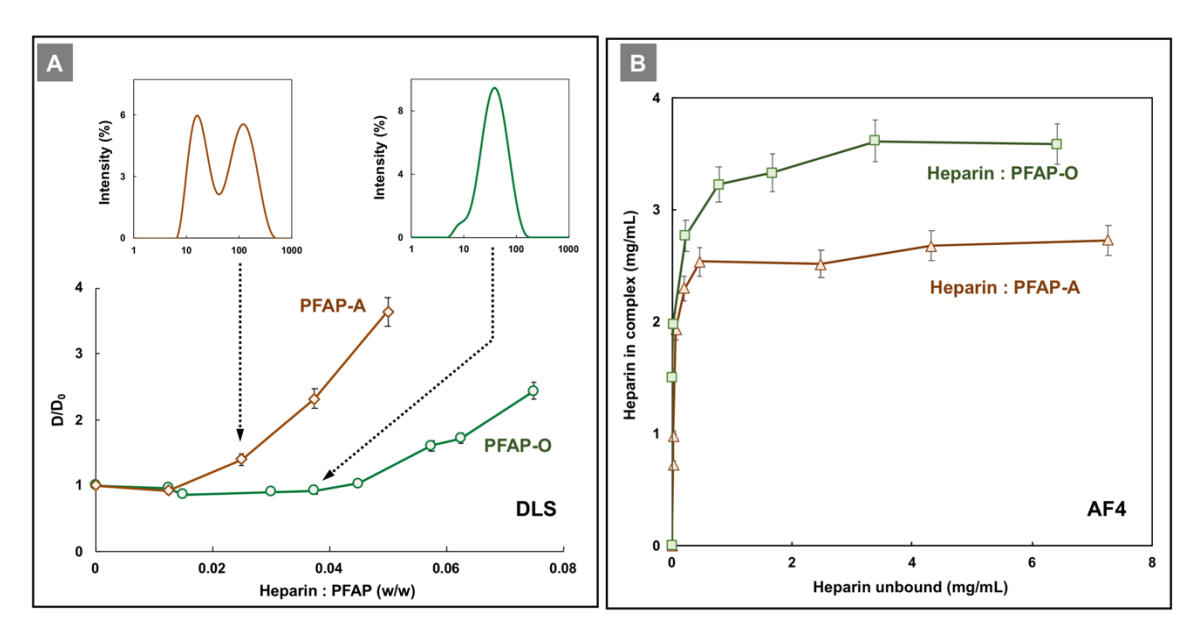


Figure 2. (A) Hydrodynamic diameters of heparin-polymer formulations vs their compositions as monitored by DLS (relative changes in diameter (D/D₀) shown: D - z-average hydrodynamic diameter of formulation; D₀ - z-average hydrodynamic diameter of the polymer; insets show DLS profiles by intensity for formulations indicated by dashed arrows: 0.025 and 0.038 for heparin-to-polymer weight ratios for PFAP-A and PFAP-O, correspondingly); (B) isotherms of binding for heparin-polymer systems calculated from measurements of unbound heparin concentration in the system by AF4 method (10 mM phosphate buffer; pH 5; error bars indicate standard deviation).

Preparation and Characterization of Heparin-Containing Fluoro-Coatings Using LbL Nanoassembly.

Because PFAP-O appeared to be less susceptible to agglomeration in solution and uptake more heparin in complexes, we selected PFAP-O for further LbL nanoassembly with heparin. LbL coatings of PFAP-O and heparin were assembled on silicon wafers at pH 5, 7.5, and 8 to compare their assembly at surfaces to their complexation in solution. The thicknesses of the dry films were monitored up to five bilayers using spectroscopic ellipsometry, as shown in **Figure 3A.** In this Figure, the growth of (PFAP-O/Heparin) coatings from pH 7.5 solutions appears to be nearly linear, indicating strong, stable interactions between the anion and polycation layers. In contrast, the growth at pH 8 shows random growth and loss, possibly due to the

reduced charge on PFAP-O leading to agglomeration and eventual desorption of the weakly bound layers. Furthermore, at pH 5, the coatings appeared to stay at a constant thickness, indicating a lack of adsorption of the heparin and PFAP-O during subsequent depositions. At pH 5, the increased density of positive charge on PFAP-O may increase the hydrophilicity of the PFAP-O+heparin complexes, ultimately favoring complex formation in solution above the surface rather than at the surface and therefore leading to a lack of film growth.

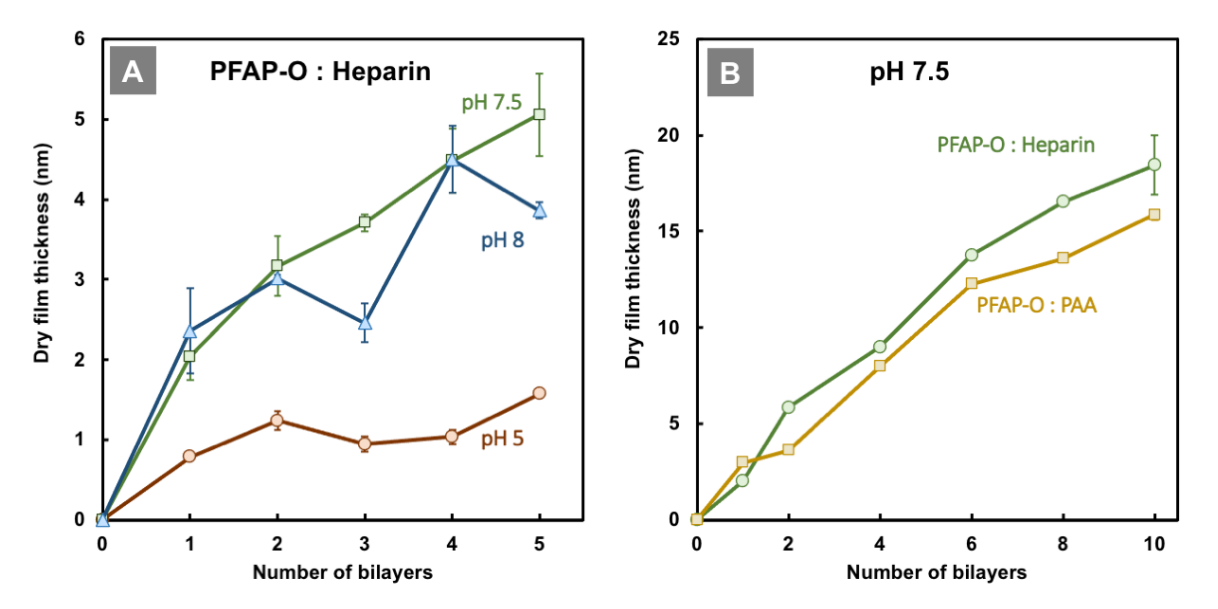


Figure 3. (A) Thickness as a function of number of bilayers for PFAP-O and heparin LbL coatings (PFAP-O: Heparin) deposited from pH 5, 7.5, and 8, as measured by spectroscopic ellipsometry. **(B)** Film growth curves up to 10 bilayers for PFAP-O assembled with heparin or poly(acrylic acid), i.e. (PFAP-O: Heparin) or (PFAP-O: PAA), from solutions at pH 7.5, as measured by spectroscopic ellipsometry.

Using the optimal pH 7.5 deposition conditions, PFAP-O was assembled with heparin or poly(acrylic acid), PAA on silicon and titanium substrates. The thicknesses of the coatings were measured every two bilayers using spectroscopic ellipsometry, as shown in Figure 3B. In this Figure, both (PFAP-O/Heparin) and (PFAP-O/PAA) coatings were shown to grow linearly up to 10 bilayers, averaging ~2 nm growth per bilayer. The growth results on the titanium substrate were similar, which is consistent with previous

findings.¹⁵ All coatings were terminated with either heparin or poly(acrylic acid) for further thrombogenicity testing. Additionally, the static water contact angle of the heparin-capped coatings increased from 17° at 5 bilayers to 30° at 10 bilayers even though the highly hydrophilic heparin was present at the solid-liquid interface (Figure S8). This increase in hydrophobicity with film thickness is an important factor that may be used to design the surface wetting of a film regardless of the capping layer, achieving a specific wettability needed for biomedical devices.

In Vitro Thrombogenicity Evaluation of Coatings – Heparin-containing Fluorinated Nanofilms Display Reduced Thrombin Formation and Platelet Adhesion, While Maintaining Low Hemolytic Activity. The thrombogenicity of a surface remains one of the main reasons for the failure of blood-contacting implants and devices^{1, 2, 4} and the examination of material-induced thrombosis is an important requirement under a guidance developed by the International Organization for Standardization (ISO 10993-4).^{2, 42} Therefore, the key test categories for in vitro evaluation of biomaterials with fresh human blood usually encompass assessment of hemolysis, adhesion and activation of platelets, and initiation of intrinsic coagulation pathway by contact activation.^{2, 3, 43}

Thrombin generation assay (TGA), which measures enzymatic activity of thrombin photometrically or fluorometrically, is noted to be the most direct and reproducible test for evaluating activity level of the coagulation system. Thrombin is a key protease in the coagulation cascade, which cleaves plasma protein fibrinogen into fibrin monomers eventually leading to the formation of polymerized fibrin clot, and also serves as a platelet activator promoting their local aggregation. Because the activity of thrombin is regulated by an antithrombin—heparin inhibitory mechanism, this assay can be also informative on the availability of heparin in the coatings.

The evaluation of heparin-containing fluorinated surfaces was carried out using LbL coatings deposited on titanium wafers. Test articles were incubated with citrated plasma obtained from whole Human blood and the activity of thrombin was measured at discrete time intervals using a fluorogenic substrate.³⁰ The

results were benchmarked against those for a non-heparinized fluorinated coating assembled using PAA and an uncoated titanium sample (**Figure 4A**). As seen from the Figure, the sample with a heparinized coating displayed dramatically lower thrombin generation activity, which is consistent with the availability of this indirect thrombin inhibitor on the surface of this material.

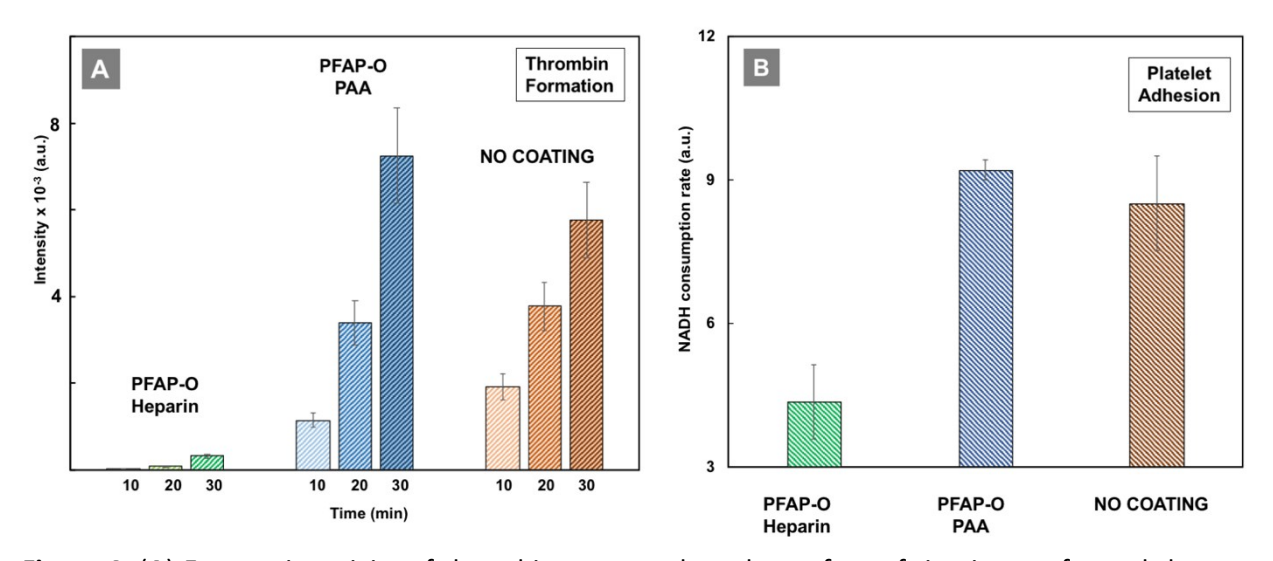


Figure 4. (**A**) Enzymatic activity of thrombin generated on the surface of titanium wafer and the same material coated with PFAP-O: heparin and PFAP-O: PAA vs sample incubation time (citrated Human plasma, 37°C, thrombin formation induced by calcium chloride; n=2; errors represent standard deviation); (**B**) NADH consumption on the same materials, which is proportional to LDH activity of surfaced retained and then lysed platelets (platelet rich plasma from whole human blood; 37°C, lactate dehydrogenase assay; n=2; errors represent standard deviation).

Another important key to understanding thrombogenicity of a biomaterial is the way its surface interacts with platelets, which, along with fibrin, constitutes one of the two main components of thrombi.^{2, 4} This parameter appears to be particularly important for fluorinated materials, as the failure of polytetrafluoroethylene (PTFE)-based vascular grafts has been largely associated with platelet-mediated thrombosis.⁴⁶ To reduce platelet adhesion, studies have been reported on chemical modification of fluoropolymers with peptides, polysaccharides, and hydrophilic polymers.^{13, 46}

The number of platelets retained by surfaces of tested materials was evaluated on the basis of enzymatic activity of lactate dehydrogenase (LDH), which is released after surfactant-induced lysis of surface-adhered cells.^{30, 47} NADH consumption in LDH-catalyzed conversion of pyruvate to lactate in this assay is proportional to platelet retention on the surface. **Figure 4B** shows that the non-heparinized PFAP-O+PAA coating is characterized by LDH activity (NADH consumption), which is similar to that for the uncoated titanium. In contrast, enzymatic activity of lysate obtained using PFAP-O+heparin surface is significantly lower, which indicates reduced counts of platelets retained by the heparin-functionalized coating.

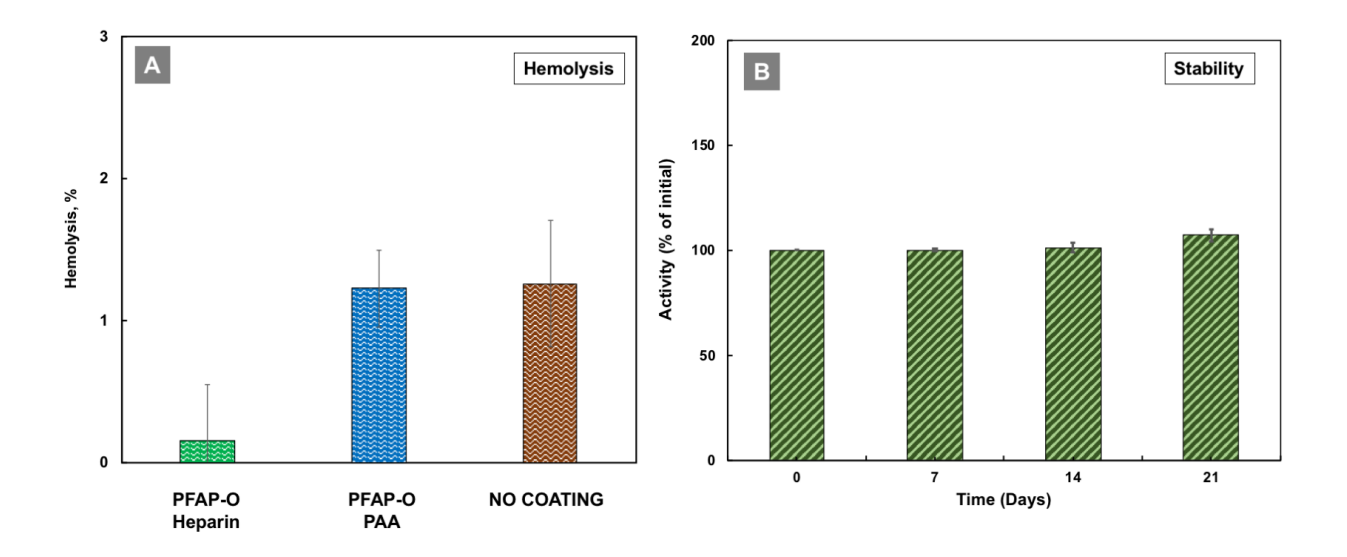


Figure 5. (A) Hemolysis of diluted human blood on the surfaces of coated and uncoated titanium samples (37°C; 4 h; n=2; errors represent standard deviation); (B) Anticoagulant activity of heparin-coated titanium samples after their incubation in aqueous solutions as assessed by TGA (37°C, pH 7.4, PBS; anticoagulation activity of samples, which were not exposed to PBS (time = 0), is shown as 100%; n=2, average values shown, error bars represent standard deviation).

Material surfaces in contact with blood can cause hemolysis - rupturing of red blood cells with release of intracellular molecules. Released hemoglobin can in turn lead to a number of undesirable outcomes, such as platelet activation, conversion of prothrombin to thrombin, as well as expression of adhesion

molecules resulting in vessel obstruction and tissue hypoxia.² Therefore, hemolysis assays constitute one of the most important categories in testing biomaterials with free hemoglobin in diluted human plasma considered to be a classical analyte.^{2,3} Hemolysis of diluted human blood on coated and uncoated titanium samples was evaluated at 37°C for 4 h using a modified American Society for Testing and Materials (ASTM) method.³¹ Although, once again, the results for non-heparinized fluorinated surface and uncoated titanium were similar, the percent of hemolysis for heparin-containing sample was lower (**Figure 5A**).

Development of non-eluting heparin coating technologies is an important approach to conferring long-term surface thromboresistance. To that end, permanent immobilization of heparin appears to be preferred, as, contrary to coatings allowing for the release of polysaccharide over time, non-eluting coatings are not expected to impact clotting in the bulk therefore preventing systemic anticoagulant effects. Thus, heparin-containing polyphosphazene coatings were assessed for stability in a near-physiological environment. Their anticoagulant activity was evaluated after various periods of exposure to PBS (pH 7.4) using a TGA assay. No noticeable changes in anticoagulant activity of coatings were detected, which indicates that heparin maintained its association with the coating for at least a three-week period (Figure 5B). These results are also consistent with the high stability of heparin-polymer complexes determined on the basis of isotherms of binding (Figure 2B) and suggest that fluoropolymer-based LbL assemblies provide an alternative option for the development of non-eluting heparin-containing coatings.

CONCLUSIONS

The development of effective and safe material surfaces, which can eliminate device thrombogenicity, remains one of the prevailing challenges in the field of biomaterials. Due to their omniphobic properties and high durability, fluoropolymers present some of the optimal and highly desirable choices for designing blood-contacting biomaterials. However, due to their insolubility in water, the absolute majority of polymers containing fluorinated groups are not compatible with aqueous based anticoagulants, such as

polysaccharides (heparin, fondaparinux), peptides (hirudine, lepirudin), or proteins (antithrombin).

Water-soluble fluorinated polyphosphazene polyelectrolytes, such as PFAP-O introduced in the present

paper, enable the development of all-aqueous formulations with such agents and allow their assembly

into coatings using a LbL technique. In vitro thrombogenicity studies demonstrated that non-covalent

incorporation of heparin into the LbL assembled fluorinated nanocoatings resulted in a dramatic reduction

of antithrombotic activity while maintaining excellent hemocompatibility. It is envisioned that this simple

approach, which avoids sophisticated pathways for covalent attachment of heparin to material surface

and allows for precise control of nanocoatings, can be applied to a wide spectrum of therapeutically

important ionic molecules.

ASSOCIATED CONTENT

Supporting Information.

The Supporting Information is available free of charge.

¹H and ³¹P NMR spectra of PFAP-O and PFAP-A; DLS profiles of polymers and molecular mass standards

with calibration curves; AF4 fractograms of polymers and molecular mass standards with calibration

curves; AF4 fractograms of heparin-PFAP-O solution formulations; results of static water contact angle

measurements on different coatings.

AUTHOR INFORMATION

Corresponding author

Alexander K. Andrianov: *E-mail: aandrianov@umd.edu

Author Contributions

The manuscript was written through contributions of all authors. All authors have given approval to the

final version of the manuscript.

20

Acknowledgment

This work was supported by the National Science Foundation under Award DMR-1808483 (S.S.) and DMR-1808531 (A.A.)

ABBREVIATIONS

LbL, layer-by-layer; PFAP-O, poly[(trifluoroethoxy)(dimethylaminopropyloxy)phosphazene]; PFAP-A, poly[(trifluoroethoxy)(dimethylaminopropylamino)phosphazene]; NADH, nicotinamide adenine dinucleotide, reduced disodium salt hydrate; PDCP, polydichlorophosphazene; DLS, dynamic light scattering; LDH, lactate dehydrogenase; PRP, platelet rich plasma; ISO, International Organization for Standardization; TGA, thrombin generation assay; PAA, poly(acrylic acid); PTFE, polytetrafluoroethylene; ASTM, American Society for Testing and Materials.

REFERENCES

- 1. Labarrere, C. A.; Dabiri, A. E.; Kassab, G. S., Thrombogenic and Inflammatory Reactions to Biomaterials in Medical Devices. Front. Bioeng. Biotechnol. 2020, 8, 123, doi: 10.3389/fbioe.2020.00123.
- 2. Braune, S.; Latour, R. A.; Reinthaler, M.; Landmesser, U.; Lendlein, A.; Jung, F., In Vitro Thrombogenicity Testing of Biomaterials. Adv. Healthcare Mater. 2019, 8, (21), 1900527.
- 3. Weber, M.; Steinle, H.; Golombek, S.; Hann, L.; Schlensak, C.; Wendel, H. P.; Avci-Adali, M., Blood-Contacting Biomaterials: In Vitro Evaluation of the Hemocompatibility. Front. Bioeng. Biotechnol. 2018, 6, 99, doi: 10.3389/fbioe.2018.00099.
- 4. Jaffer, I. H.; Fredenburgh, J. C.; Hirsh, J.; Weitz, J. I., Medical device-induced thrombosis: what causes it and how can we prevent it? J. Thromb. Haemostasis 2015, 13, (S1), S72-S81.
- 5. Biran, R.; Pond, D., Heparin coatings for improving blood compatibility of medical devices. Adv. Drug Delivery Rev. 2017, 112, 12-23.

- 6. Linhardt, R. J.; Murugesan, S.; Xie, J., Immobilization of heparin: approaches and applications. Curr. Top. Med. Chem. 2008, 8, (2), 80-100.
- 7. Decher, G.; Hong, J.-D., Buildup of ultrathin multilayer films by a self-assembly process, 1 consecutive adsorption of anionic and cationic bipolar amphiphiles on charged surfaces. Makromol. Chem., Macromol. Symp. 1991, 46, (1), 321-327.
- 8. Elahi, M. F.; Guan, G.; Wang, L.; Zhao, X.; Wang, F.; King, M. W., Surface Modification of Silk Fibroin Fabric Using Layer-by-Layer Polyelectrolyte Deposition and Heparin Immobilization for Small-Diameter Vascular Prostheses. Langmuir 2015, 31, (8), 2517-2526.
- 9. Bates, M. C.; Yousaf, A.; Sun, L.; Barakat, M.; Kueller, A., Translational Research and Early Favorable Clinical Results of a Novel Polyphosphazene (Polyzene-F) Nanocoating. Regen. Eng. Transl. Med. 2019, 1-13.
- 10. Gardiner, J., Fluoropolymers: Origin, Production, and Industrial and Commercial Applications. Aust. J. Chem. 2015, 68, (1), 13-22.
- 11. Teo, A. J. T.; Mishra, A.; Park, I.; Kim, Y.-J.; Park, W.-T.; Yoon, Y.-J., Polymeric Biomaterials for Medical Implants and Devices. ACS Biomater. Sci. Eng. 2016, 2, (4), 454-472.
- 12. Wang, A.; Cao, T.; Tang, H.; Liang, X.; Black, C.; Salley, S. O.; McAllister, J. P.; Auner, G. W.; Ng, K. Y. S., Immobilization of polysaccharides on a fluorinated silicon surface. Colloids Surf., B 2006, 47, (1), 57-63.
- 13. Gao, Q.; Chen, Y.; Wei, Y.; Wang, X.; Luo, Y., Heparin-grafted poly(tetrafluoroethylene-co-hexafluoropropylene) film with highly effective blood compatibility via an esterification reaction. Surf. Coat. Technol. 2013, 228, S126-S130.
- 14. Albright, V.; Penarete-Acosta, D.; Stack, M.; Zheng, J.; Marin, A.; Hlushko, H.; Wang, H.; Jayaraman, A.; Andrianov, A. K.; Sukhishvili, S. A., Polyphosphazenes enable durable, hemocompatible, highly efficient antibacterial coatings. Biomaterials 2021, 268, 120586.

- 15. Selin, V.; Albright, V.; Ankner, J. F.; Marin, A.; Andrianov, A. K.; Sukhishvili, S. A., Biocompatible Nanocoatings of Fluorinated Polyphosphazenes through Aqueous Assembly. ACS Appl. Mater. Interfaces 2018, 10, (11), 9756-9764.
- 16. Albright, V.; Marin, A.; Kaner, P.; Sukhishvili, S. A.; Andrianov, A. K., New Family of Water-Soluble Sulfo–Fluoro Polyphosphazenes and Their Assembly within Hemocompatible Nanocoatings. ACS Appl. Bio Mater. 2019, 2, (9), 3897-3906.
- 17. Weir, M. D.; Kaner, P.; Marin, A.; Andrianov, A. K., Ionic Fluoropolyphosphazenes as Potential Adhesive Agents for Dental Restoration Applications. Regener. Eng. Transl. Med. 2021, 7, (1), 10-20.
- 18. Albright, V.; Selin, V.; Hlushko, H.; Palanisamy, A.; Marin, A.; Andrianov, A. K.; Sukhishvili, S. A., Fluorinated Polyphosphazene Coatings Using Aqueous Nano-Assembly of Polyphosphazene Polyelectrolytes. In Polyphosphazenes in Biomedicine, Engineering, and Pioneering Synthesis, American Chemical Society: 2018; Vol. 1298, pp 101-118.
- 19. Andrianov, A. K.; Marin, A.; Peterson, P.; Chen, J., Fluorinated polyphosphazene polyelectrolytes. J. Appl. Polym. Sci. 2007, 103, (1), 53-58.
- 20. Zhang, Z.; Shen, W.; Ling, J.; Yan, Y.; Hu, J.; Cheng, Y., The fluorination effect of fluoroamphiphiles in cytosolic protein delivery. Nat. Commun. 2018, 9, (1), 1377.
- 21. Xu, J.; Lv, J.; Zhuang, Q.; Yang, Z.; Cao, Z.; Xu, L.; Pei, P.; Wang, C.; Wu, H.; Dong, Z.; Chao, Y.; Wang, C.; Yang, K.; Peng, R.; Cheng, Y.; Liu, Z., A general strategy towards personalized nanovaccines based on fluoropolymers for post-surgical cancer immunotherapy. Nat. Nanotechnol. 2020, 15, (12), 1043-1052.
- 22. Tan, E.; Lv, J.; Hu, J.; Shen, W.; Wang, H.; Cheng, Y., Statistical versus block fluoropolymers in gene delivery. J. Mater. Chem. B 2018, 6, (44), 7230-7238.
- 23. Lin, J.; Chen, X.; Chen, C.; Hu, J.; Zhou, C.; Cai, X.; Wang, W.; Zheng, C.; Zhang, P.; Cheng, J.; Guo, Z.; Liu, H., Durably Antibacterial and Bacterially Antiadhesive Cotton Fabrics Coated by Cationic Fluorinated Polymers. ACS Appl. Mater. Interfaces 2018, 10, (7), 6124-6136.

- 24. Lee, C.-Y.; Ha, J.-W.; Jun Park, I.; Lee, S.-B., Surface characteristics of water-soluble cationic fluoro copolymers containing perfluoroalkyl, quaternized amino, and hydroxyl groups. J. Appl. Polym. Sci. 2002, 86, (14), 3702-3707.
- 25. Allcock, H. R.; McIntosh, M. B.; Klingenberg, E. H.; Napierala, M. E., Functionalized Polyphosphazenes: Polymers with Pendent Tertiary Trialkylamino Groups. Macromolecules 1998, 31, (16), 5255-5263.
- 26. Wang, M.; Liu, H.; Li, L.; Cheng, Y., A fluorinated dendrimer achieves excellent gene transfection efficacy at extremely low nitrogen to phosphorus ratios. Nat. Commun. 2014, 5, (1), 3053.
- 27. Andrianov, A. K.; Chen, J.; LeGolvan, M. P., Poly(dichlorophosphazene) as a precursor for biologically active polyphosphazenes: Synthesis, characterization, and stabilization. Macromolecules 2004, 37, (2), 414-420.
- 28. Kozlovskaya, V.; Yakovlev, S.; Libera, M.; Sukhishvili, S. A., Surface Priming and the Self-Assembly of Hydrogen-Bonded Multilayer Capsules and Films. Macromolecules 2005, 38, (11), 4828-4836.
- 29. Selin, V.; Albright, V.; Ankner, J. F.; Marin, A.; Andrianov, A. K.; Sukhishvili, S. A., Biocompatible Nanocoatings of Fluorinated Polyphosphazenes through Aqueous Assembly. ACS Applied Materials & Interfaces 2018, 10, (11), 9756-9764.
- 30. Sperling, C.; Fischer, M.; Maitz, M. F.; Werner, C., Blood coagulation on biomaterials requires the combination of distinct activation processes. Biomaterials 2009, 30, (27), 4447-4456.
- 31. Henkelman, S.; Rakhorst, G.; Blanton, J.; van Oeveren, W., Standardization of incubation conditions for hemolysis testing of biomaterials. Mater. Sci. Eng.: C Mater. Biol. Appl. 2009, 29, (5), 1650-1654.
- 32. Luten, J.; Van Steenis, J. H.; Van Someren, R.; Kemmink, J.; Schuurmans-Nieuwenbroek, N. M. E.; Koning, G. A.; Crommelin, D. J. A.; Van Nostrum, C. F.; Hennink, W. E., Water-soluble biodegradable cationic polyphosphazenes for gene delivery. J. Controlled Release 2003, 89, (3), 483-497.

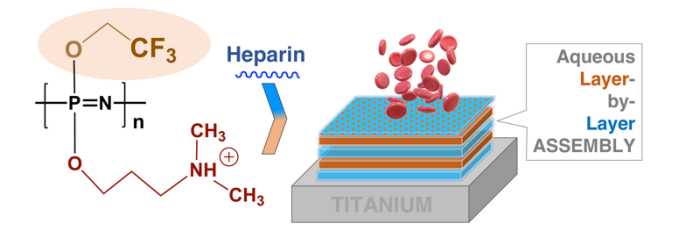
- 33. Vajihinejad, V.; Gumfekar, S. P.; Dixon, D. V.; Silva, M. A.; Soares, J. B. P., Enhanced dewatering of oil sands tailings by a novel water-soluble cationic polymer. Sep. Purif. Technol. 2021, 260, 118183.
- 34. Vajihinejad, V.; Gumfekar, S. P.; Bazoubandi, B.; Rostami Najafabadi, Z.; Soares, J. B. P., Water Soluble Polymer Flocculants: Synthesis, Characterization, and Performance Assessment. Macromol. Mater. Eng. 2019, 304, (2), 1800526.
- 35. Andrianov, A. K.; Le Golvan, M. P., Characterization of poly[di(carboxylatophenoxy)-phosphazene] by an aqueous gel permeation chromatography. J. Appl. Polym. Sci. 1996, 60, (12), 2289-2295.
- 36. Liu, Y.; Bo, S.; Zhu, Y.; Zhang, W., Determination of molecular weight and molecular sizes of polymers by high temperature gel permeation chromatography with a static and dynamic laser light scattering detector. Polymer 2003, 44, (23), 7209-7220.
- 37. Stetefeld, J.; McKenna, S. A.; Patel, T. R., Dynamic light scattering: a practical guide and applications in biomedical sciences. Biophys. Rev. 2016, 8, (4), 409-427.
- 38. Messaud, F. A.; Sanderson, R. D.; Runyon, J. R.; Otte, T.; Pasch, H.; Williams, S. K. R., An overview on field-flow fractionation techniques and their applications in the separation and characterization of polymers. Prog. Polym. Sci. 2009, 34, (4), 351-368.
- 39. Pitkänen, L.; Striegel, A. M., AF4/MALS/QELS/DRI characterization of regular star polymers and their "span analogs". Analyst 2014, 139, (22), 5843-5851.
- 40. Allcock, H. R.; Kim, Y. B., Synthesis, Characterization, and Modification of Poly(organophosphazenes) with Both 2,2,2-Trifluoroethoxy and Phenoxy Side Groups. Macromolecules 1994, 27, (14), 3933-3942.
- 41. Kuriyan, J.; Konforti, B.; Wemmer, D., The molecules of life: Physical and chemical principles.

 Garland Science: New York, NY and London, 2012; p 1008.
 - 42. International Organization for Standardization (2000). Biological Evaluation of

Medical Devices. https://www.iso.org/standard/63448.html (August 26, 2021),

- 43. Seyfert, U. T.; Biehl, V.; Schenk, J., In vitro hemocompatibility testing of biomaterials according to the ISO 10993-4. Biomol. Eng. 2002, 19, (2), 91-96.
- 44. Van Oeveren, W.; Haan, J.; Lagerman, P.; Schoen, P., Comparison of Coagulation Activity Tests In Vitro for Selected Biomaterials. Artif. Organs 2002, 26, (6), 506-511.
- 45. Müller, J.; Becher, T.; Braunstein, J.; Berdel, P.; Gravius, S.; Rohrbach, F.; Oldenburg, J.; Mayer, G.; Pötzsch, B., Profiling of Active Thrombin in Human Blood by Supramolecular Complexes. Angew. Chem. Int. Ed. 2011, 50, (27), 6075-6078.
- 46. Tang, C.; Kligman, F.; Larsen, C. C.; Kottke-Marchant, K.; Marchant, R. E., Platelet and endothelial adhesion on fluorosurfactant polymers designed for vascular graft modification. J. Biomed. Mater. Res. A 2009, 88, (2), 348-358.
- 47. Tamada, Y.; Kulik, E. A.; Ikada, Y., Simple method for platelet counting. Biomaterials 1995, 16, (3), 259-261.

FLUOROPOLYMER NANOCOATINGS with ANTICOAGULANT activity



For Table of Contents Only